

DIGITAL ACCESS TO SCHOLARSHIP AT HARVARD
DASH.HARVARD.EDU

HARVARD LIBRARY


Black carbon and its correlation with trace gases at a rural site in Beijing: Top-down constraints from ambient measurements on bottom-up emissions

Citation

Wang, Yuxuan, Xuan Wang, Yutaka Kondo, Mizuo Kajino, J. William Munger, and Jiming Hao. 2011. “Black Carbon and Its Correlation with Trace Gases at a Rural Site in Beijing: Top-down Constraints from Ambient Measurements on Bottom-up Emissions.” J. Geophys. Res. 116 (D24) (December 27). doi:10.1029/2011jd016575.

Published version

https://doi.org/10.1029/2011JD016575

Link

http://nrs.harvard.edu/urn-3:HUL.InstRepos:28347436

Terms of use

This article was downloaded from Harvard University’s DASH repository, and is made available under the terms and conditions applicable to Other Posted Material (LAA), as set forth at

https://harvardwiki.atlassian.net/wiki/external/NGY5NDE4ZjgzNTc5NDQzMGIzZWZhMGFlOWI2M2EwYTg

Accessibility

https://accessibility.huit.harvard.edu/digital-accessibility-policy

Share Your Story

The Harvard community has made this article openly available.
Please share how this access benefits you. Submit a story

Black carbon and its correlation with trace gases at a rural site in Beijing: Top-down constraints from ambient measurements on bottom-up emissions

Yuxuan Wang,[1] Xuan Wang,[2] Yutaka Kondo,[3] Mizuo Kajino,[4] J. William Munger,[5] and Jiming Hao[1,2]

Received 18 July 2011; revised 2 October 2011; accepted 18 October 2011; published 28 December 2011.

[1] The mass concentrations of black carbon (BC) were measured continuously at Miyun, a rural site near Beijing, concurrently with some trace gases (CO, CO_2, NO_y, SO_2) during the nonheating seasons of 2010 (April to October). The average concentration of BC was 2.26 ± 2.33 μg m^{-3}. About 70%–100% of the air masses arriving at the site from June to September were from the source region of Beijing and the North China Plain (NCP), while in the spring, 40% were of continental background origin. BC had moderate to strong positive correlations with CO (R^2 = 0.51), NO_y (R^2 = 0.58), and CO_2 (nonsummer, R^2 = 0.54), but not with SO_2 (R^2 < 0.1). The observed ΔBC/ΔCO ratio was 0.0050 ± 0.0001 μg m^{-3}/ppbv for the regional air masses (excluding the influence of biomass burning). This ratio increased by 68% to 0.0084 ± 0.0004 μg m^{-3}/ppbv after excluding the influence of wet deposition. Accounting further for the impact of atmospheric processes on the observation, we derived an average top-down BC/CO emission ratio of 0.0095 ± 0.002 μg m^{-3}/ppbv for the source region of Beijing and NCP that is 18%–21% lower than the average emission ratio from the bottom-up inventory of Zhang et al. (2009), whereas the difference is substantially lower than the uncertainty of emissions for either species. The difference between the mean bottom-up and top-down emission ratios is most likely to be attributed to the residential sector, which needs to have a lower share in the total emissions of BC or a much lower BC/CO emission ratio. The industry and transportation sectors are found to be dominant sources of BC from Beijing and the NCP rather than from the residential sector as suggested by the bottom-up inventory.

Citation: Wang, Y., X. Wang, Y. Kondo, M. Kajino, J. W. Munger, and J. Hao (2011), Black carbon and its correlation with trace gases at a rural site in Beijing: Top-down constraints from ambient measurements on bottom-up emissions, *J. Geophys. Res.*, *116*, D24304, doi:10.1029/2011JD016575.

1. Introduction

[2] Black carbon (BC), consisting of a variety of different forms of pure carbon, is an important component of airborne particulate matter (PM). Major sources of BC are the incomplete combustion of fossil fuel and biomass, including forest fires [*Penner et al.*, 1993; *Masiello*, 2004; *Cooke et al.*, 1999]. On the local scale, BC is associated with adverse effects on public health by absorbing harmful VOCs such as polycyclic aromatic hydrocarbons (PAHs) [*Dachs and Eisenreich*, 2000]. BC has a warming effect on the atmosphere by intercepting and absorbing sunlight [*Jacobson*, 2001; *Myhre et al.*, 1998; *Solomon et al.*, 2007; *Ramanathan and Carmichael*, 2008]. As BC remains in the atmosphere for only days, the effect of BC on climate depends critically on its temporal and spatial variations. On the global scale, the mean direct radiative forcing of BC is estimated to be 0.34 ± 0.25 W m^{-2} [*Solomon et al.*, 2007]. The deposition of BC on snow and ice reduces surface albedo and consequently results in acceleration of melting, for example, over the Himalayan glaciers and the Arctic ice [*Ramanathan and Carmichael*, 2008; *Solomon et al.*, 2007]. BC can also affect cloud albedo by mixing with cloud condensation nuclei (CCN) and subsequently changing the hygroscopicity of CCN [*Liousse et al.*, 1996]. On the regional scale, BC can affect regional circulation and rainfall patterns by introducing significant asymmetric heating patterns [*Ramanathan et al.*, 2005]. The impact of BC on regional and global climate has not been fully quantified by models because of the lack of sufficient

[1]Ministry of Education Key Laboratory for Earth System Modeling, Center for Earth System Science, Institute for Global Change Studies, Tsinghua University, Beijing, China.
[2]School of Environment, Tsinghua University, Beijing, China.
[3]Department of Earth and Planetary Science, Graduate School of Science, University of Tokyo, Tokyo, Japan.
[4]Meteorological Research Institute, Tsukuba, Japan.
[5]Department of Earth and Planetary Sciences and School of Engineering and Applied Sciences, Harvard University, Cambridge, Massachusetts, USA.

Copyright 2011 by the American Geophysical Union.
0148-0227/11/2011JD016575

Table 1. Summary of Previous BC Measurements Around Beijing Area Together With This Study's Result

Location	Site Description	Time Period	Average BC Concentration ($\mu g/m^3$)	Measurement Method	References
Beijing	Urban area	Summer 2002	5.7	Thermal	*Dan et al.* [2004]
Beijing	Urban area	Winter 2002	15.2	Thermal	*Dan et al.* [2004]
Pinggu	Rural area	Summer 2001	4.5	Thermal	*Dan et al.* [2004]
Beijing	Urban area	Winter 2005 to January 2006	6.7	Thermal/optical	*Han et al.* [2009]
Beijing	Urban area	Spring 2006	6.2	Thermal/optical	*Han et al.* [2009]
Beijing	Urban area	Summer 2006	6.4	Thermal/optical	*Han et al.* [2009]
Beijing	Urban area	Fall 2006	8.8	Thermal/optical	*Han et al.* [2009]
Changping	Rural area	Summer 2005	2.37	Optical	*Zhou et al.* [2009]
Miyun	Rural area	Spring	1.81	Optical	This study
Miyun	Rural area	Summer	2.37	Optical	This study
Miyun	Rural area	Fall	2.41	Optical	This study

understanding of BC sources and the spatial-temporal distribution of BC in the atmosphere.

[3] It is important to understand the sources and atmospheric processes affecting the life cycle of BC in China, as China is regarded as the largest BC emitter in the world, contributing about 1/4 of the global annual total emissions of BC [*Bond et al.*, 2004; *Cooke et al.*, 1999, 2002; *Ramanathan and Carmichael*, 2008]. Previous studies have suggested that BC emissions from China were about 1.3 Tg in 1995 [*Streets et al.*, 2001], increasing to 1.1–1.5 Tg in 2000 [*Cao et al.*, 2006; *Streets et al.*, 2003a, 2003b; *Bond et al.*, 2004] and 1.8 Tg in 2006 [*Zhang et al.*, 2009]. Coal burning and biofuel combustion are major sources of BC in China. Since it is very difficult to obtain accurate and representative emission factors of many types of the combustion sources, the bottom-up emission inventories may be subject to large uncertainties. Atmospheric measurements of BC in China in recent years have provided useful information about the characteristics of BC concentrations and relevant processes responsible for their variability [*Cao et al.*, 2009; *Bergin et al.*, 2001; *Cheng et al.*, 2006; *Dan et al.*, 2004; *Han et al.*, 2009; *He et al.*, 2004; *Ye et al.*, 2003; *Zhou et al.*, 2009; *Yan et al.*, 2008]. Table 1 summarizes some studies of BC observations around Beijing. Most of the measurements focused on urban areas and might not be representative of regional conditions. Only a few of these studies have attempted to evaluate BC emissions measured simultaneously with other trace species.

[4] This paper discusses the temporal variability of BC measured continuously at a rural site north of Beijing from April to October 2010. We showed in previous analyses that the site location provides an opportunity to sample both the Beijing pollution outflow and the relative clean continental background air masses flowing in from the north [*Wang et al.*, 2008, 2010]. The correlation between BC and other concurrently measured combustion tracers, including CO, CO_2, NO_y, and SO_2 provides useful "top-down" constraints on the emission estimate of BC derived from the bottom-up approach.

2. Site and Instruments

[5] The Miyun site (40°29′N, 116°46.45′E, 152 m above sea level (asl)), located about 100 km northeast of Beijing's urban center, was founded in 2004 with continuous observations of O_3, CO, CO_2, and basic meteorological data (temperature, relative humidity (RH), and wind speed and direction). Instruments to measure NO, NO_y, and SO_2 were added in 2006. Continuous BC measurement started in March 2010, and this study focuses on measurements during the non-heating seasons of 2010 (April to October). The area surrounding the Miyun site is characterized by a mix of agriculture and small villages, with no big anthropogenic emissions within a 1 km radius of the site. Winds blow mainly from the southwest, especially in spring and summer. The frequency of westerly and northeasterly winds increases in the fall. This suggests that the site is influenced by the monsoonal circulation with annual shift in wind patterns. During the study period, the average daily temperature and RH at the site were 19°C and 58%, respectively, with an average daytime wind speed of 1.3 m/s. Details of the site have been described in a previous paper [*Wang et al.*, 2008]. The location of the Miyun site is shown in Figure 1 together with anthropogenic emissions of BC and emission ratios of BC/CO in China adopted from the bottom-up emission inventory for 2006 by *Zhang et al.* [2009]. According to the bottom-up inventory, the North China Plain (NCP) region surrounding Beijing (box in Figure 1) is a major source region of BC in China. The emission ratio of BC/CO is particularly high to the southwest of Beijing, including parts of the Shanxi and Hebei provinces, where small towns with less-efficient coal combustion are located.

[6] Ambient BC concentrations are measured by a filter-based absorption photometer, the Continuous Soot Monitoring System (COSMOS), with an inlet heated to 400°C [*Miyazaki et al.*, 2008; *Kondo et al.*, 2009, 2011a]. Air is sampled at a flow rate of 16.7 L min^{-1} through an inlet equipped with a PM_1 cyclone (URG-2000-30EHB, URG Inc., Carrbo, North Carolina). The instrument monitors changes in transmittance across an automatically advancing quartz fiber filter tape at 565 nm wavelength (λ). The changes in the transmittance are converted to BC mass concentrations using the mass absorption cross section (MAC) determined by comparison with a single-particle soot photometer (SP2) based on the laser-induced incandescence (LII) technique and the thermal-optical transmittance (TOT) technique [*Kondo et al.*, 2009, 2011a]. The stability of MAC is achieved by removing volatile aerosol components before BC particles are collected on filters with the use of an inlet heated at 400°C. The BC mass concentrations are given in units of mass and volume per unit volume of air at standard temperature and pressure (STP) (273.15 K and 1013 hPa, respectively), unless otherwise stated. The accuracy of the BC mass concentrations measured by COSMOS has been estimated to be about 10% by comparison with those measured by the SP2 in Tokyo and

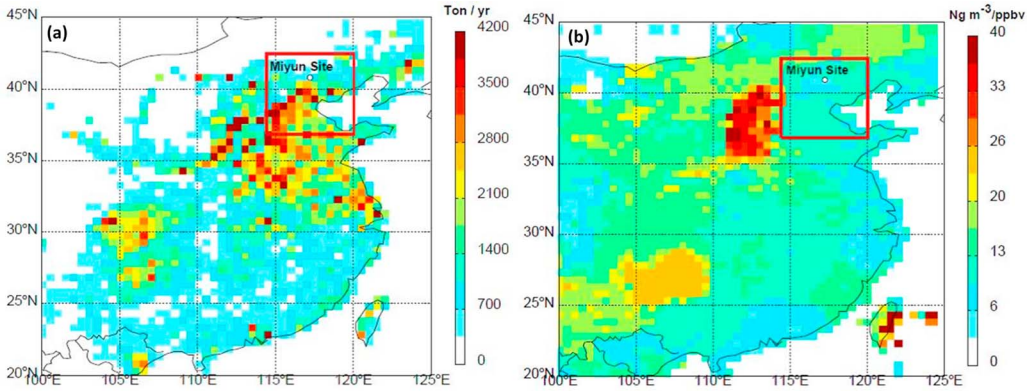


Figure 1. Location of the Miyun site (white circle). The color shading indicates (a) anthropogenic BC emissions and (b) BC/CO emission ratio in 2006 [*Zhang et al.*, 2009]. The region enclosed by the red frame represents the North China Plain, as discussed in this paper.

those with TOT instruments at six sites in Asia, including Jeju Island, which is also located downstream of the Asian continent [*Kondo et al.*, 2009, 2011a]. BC was measured with an integration time of one minute. The estimated lower limit of detection (LOD) was about 0.047 μg m^{-3}. We used 1 h average BC data for the present analysis.

[7] Mixing ratios of CO and CO_2 are detected with the gas-filter correlation infrared absorption CO analyzer (model 48C, Thermo Environmental Instruments, USA) modified for frequent external zeroing by use of a catalytic scrubber and the differential nondispersive infrared (NDIR) method (LI-COR Biosciences Li-7000). Mixing ratios of NO_y are measured by a NO-NO_y chemiluminescence analyzer (model 42C, Thermo Environmental Instruments). Mixing ratios of SO_2 are measured by the pulsed fluorescence method (model 43C, Thermo Environmental Instruments). All of these instruments have been introduced in previous papers [*Wang et al.*, 2008, 2009, 2010] and thus are not discussed here.

3. Results

[8] During the study period (April–October 2010), the average BC concentration was 2.26 μg m^{-3} with the standard deviation of 2.33 μg m^{-3}. The highest concentration was 16.77 μg m^{-3} (9 October), and the lowest was 0.03 μg m^{-3} (21 September). The measurement statistics are summarized in Table 2. The average concentration of BC at Miyun is much less than that reported previously for Chinese urban sites during the nonheating seasons (Table 1), about 70% lower in the spring and fall, 60% lower in the summer. Compared with the two rural sites near Beijing, Changping and Pinggu, listed in Table 1, the average BC concentration at Miyun in the summer (2.37 μg m^{-3}) is very similar to that at Changping (north of Beijing city, southwest of Miyun) [*Zhou et al.*, 2009], but still about 50% lower than that at Pinggu (east of Beijing city, southeast of Miyun) [*Dan et al.*, 2004]. It must be mentioned that all these other measurements around Beijing were made before 2008. Emission reduction measures taken to improve air quality during the Beijing 2008 Olympic Games [*Wang et al.*, 2009] may have reduced BC emissions, resulting in lower BC concentrations after the 2008 Olympics. Different measurement methods and particle size cuts in sampling may have caused the discrepancy in measurement results. As discussed in section 2, the BC measured by COSMOS agreed with those measured with TOT and SP2 to within about 10%.

[9] Figure 2 shows average concentrations of BC at Miyun by wind direction. High BC concentrations were mainly associated with southwesterly winds in spring and summer, while concentrations increased in northerly winds in fall. The close association of high BC with southerly winds suggests the large impact of pollution from Beijing urban areas and the NCP region located to the south on BC levels at the site.

Table 2. Summary Statistics of BC Measurements at Miyun from April to October 2010[a]

Season	Mean Value	Standard Deviation	Median Value	Maximum Value	Minimum Value
All data	2.26	2.33	1.65	16.77	0.03
Spring	1.81	1.69	1.41	7.88	0.05
Summer	2.37	1.82	1.97	12.92	0.06
Fall	2.41	2.99	1.37	16.77	0.03

[a]Units are μg/m^3.

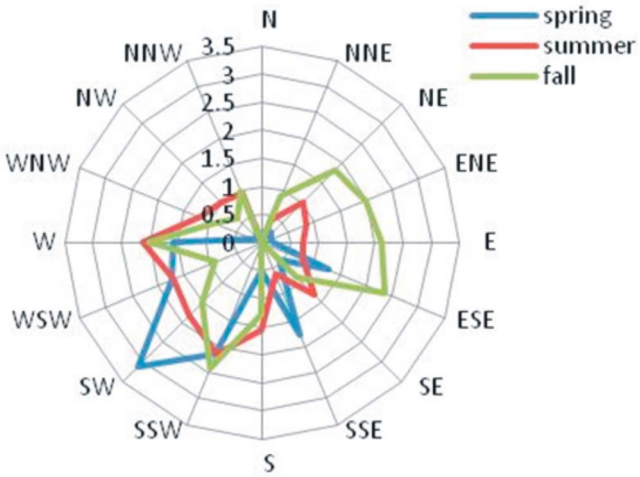


Figure 2. The median BC concentrations (units: μg m^{-3}) by wind direction and season. The numbers on the circles indicate BC concentration contours.

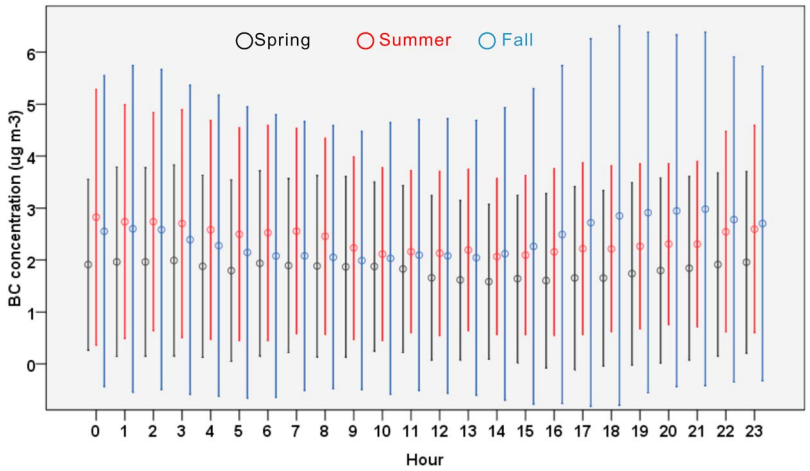


Figure 3. The mean diel cycle of BC at Miyun site. The error bars are the standard deviations.

We caution that wind directions measured at the site may not reflect the synoptic scale circulation accurately because of the influence of the site's topography. The transport patterns are discussed in section 4.2 using back trajectories.

[10] Negative correlations of aerosols with wind speeds were found in some urban areas [*Kondo et al.*, 2006; *Han et al.*, 2009; *Verma et al.*, 2010; *Ramachandran and Rajesh*, 2007] since aerosol concentrations at the surface may be

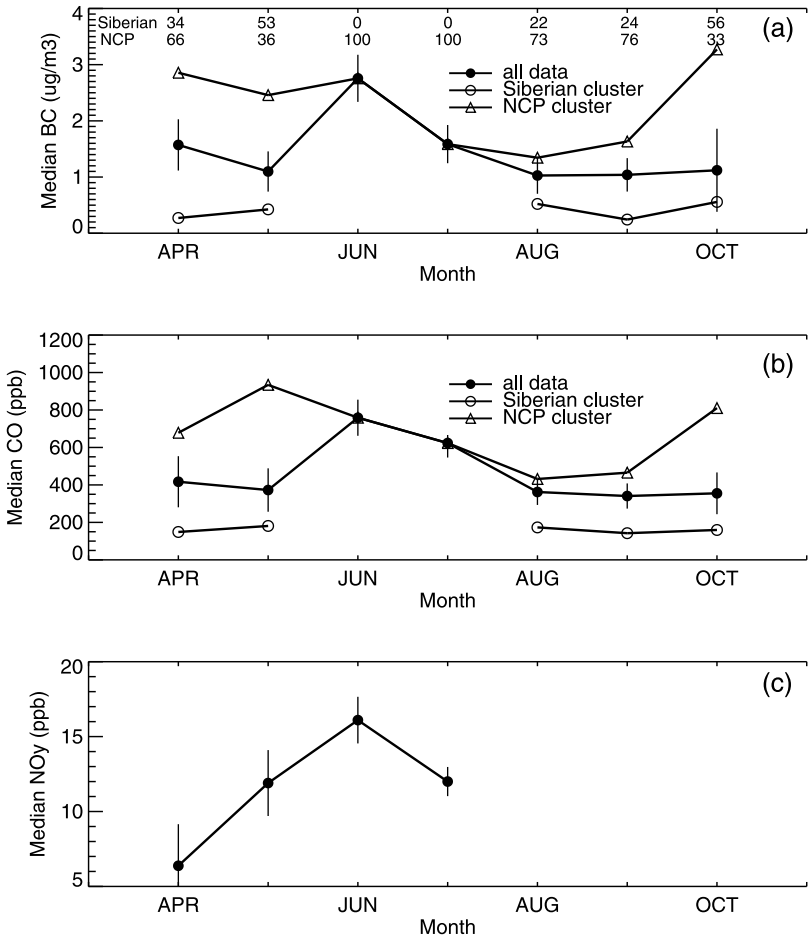


Figure 4. Monthly variations of daytime (0800–1800 LT) (a) BC, (b) CO, and (c) NO_y at the Miyun site from April to October 2010. The NO_y data were not available since late July because of the instrument failure. Median concentrations of BC and CO of the Siberian and the NCP air mass groups discussed in section 4.3 were also given. The numbers at the top of 4a are the percentages (%) of the Siberian and the NCP air masses in each month. The error bars are 1/4 of the standard deviations.

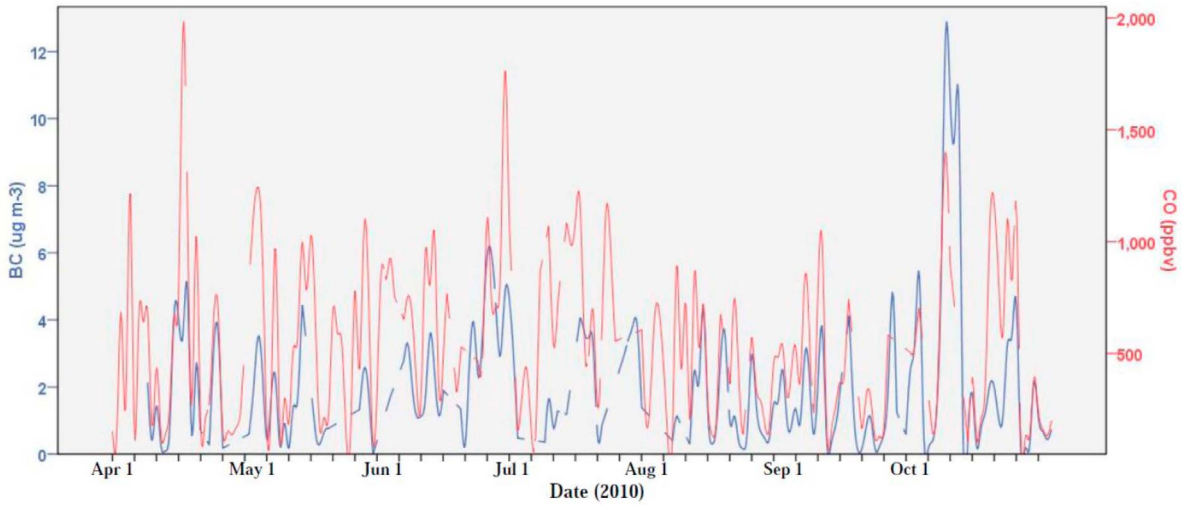


Figure 5. Time series of daytime averages (0800–1800 LT) concentrations of BC (black) and CO (red) observed at Miyun from 1 April to 1 November 2010.

lower during faster outflow of air from the source region [*Kondo et al.*, 2006]. We found no significant correlation between BC and wind speed at the Miyun site ($R^2 < 0.01$), suggesting that emissions from local sources are very limited at the site. The diurnal variation of BC is shown in Figure 3. The measurements do not show a pronounced diel cycle, although nighttime concentrations tend to be higher because of the shallow boundary layer height and lower wind speeds unfavorable for dispersion. The lack of a strong diel cycle at Miyun is in contrast to some BC measurements in urban source regions [*Han et al.*, 2009], suggesting again that BC sources are not local at Miyun. Therefore, we can use BC measurements at Miyun to examine the regional characteristics of BC concentrations and sources. Given a shallow boundary layer height and lower wind speeds at night unfavorable for pollution dispersion, nighttime observations may be more sensitive to local emissions. Therefore, we mainly focused on daytime measurements (0800 to 1800 local time), which should be more representative of regional conditions in the following discussion.

[11] Figure 4 summarizes the month-to-month variations in median daytime concentrations of BC at Miyun. For comparison, mixing ratios of CO and NO_y concurrently measured at the site are also shown. The month-to-month variability of BC is similar to that of CO and NO_y, indicating that the sources of these species are collocated and/or their variances are affected by the same atmospheric transport to the site. Concentrations of all the species peak in June, followed by a minimum in August. Concentrations increase again in autumn. The peak of all the pollutants in June can be explained by increased frequency of southwest outflow from the Beijing urban area along with crop residue burning following the harvest of winter wheat. According to the daily reports of satellite-derived straw-burning monitoring from the Ministry of Environmental Protection of China (http://hjj.mep.gov.cn/stjc/), there was a total of 70 fire spots surrounding Beijing observed in June, whereas no fire spots were found in other months. Figure 5 shows the time series of daytime average concentrations of BC and CO observed at Miyun from 1 April to 1 November 2010. The highest peak of BC was in early October, which will be discussed later. Both BC and CO concentrations exhibit sharp increases every 4 to 10 days. This phenomenon cannot be caused only by emissions. Meteorological conditions such as frontal passages may result in this cycle, as suggested by *Jia et al.* [2008] in their analysis of $PM_{2.5}$ measurements in Beijing.

[12] Figure 6 shows the frequency distribution of daytime BC concentrations by season. The distribution shows a pronounced peak of about 0.11 μg m^{-3} in both spring and fall and a long tail toward higher concentrations. The distribution in summer is flatter, with minor peaks at about 0.16 and 0.6 μg m^{-3}. The higher peak indicates that the summertime measurements may reflect more polluted air masses from the polluted regions to the south. High concentrations of BC in October were caused mainly by a pollution episode occurring from 6 to 10 October. The daily air quality reports provided by the Ministry of Environmental Protection of China (http://datacenter.mep.gov.cn) identified the four days between 6 and 9 October as heavily polluted days. From Figure 5, we can find that both BC and CO showed a sharp, concurrent

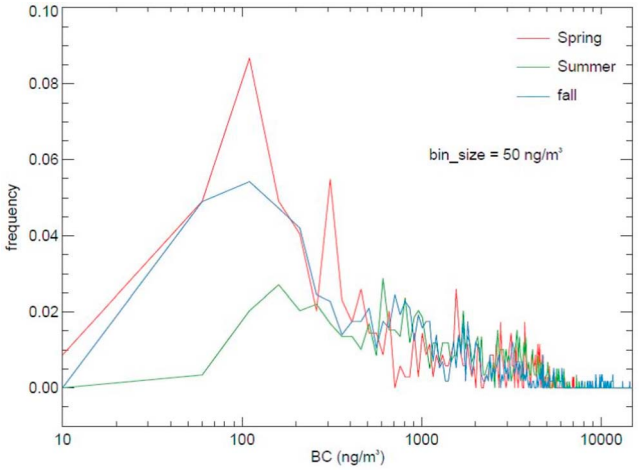


Figure 6. The frequency distribution of daytime BC concentrations by season.

Table 3. Mean and Standard Deviation of Species Concentration and Meteorological Parameters During the Pollution Episode From 6 to 8 October 2010

Period	BC (μg m^{-3})	CO (ppb)	CO_2 (ppm)	Wind Speed (m/s)	Temperature (°C)	Relative Humidity (%)
Pollution episode (6–8 October)	11.45 ± 2.55	1335.0 ± 370.6	438.6 ± 12.9	0.89 ± 0.81	16.7 ± 2.9	72.9 ± 14.1
Other data in October	3.74 ± 0.52	473.4 ± 30.2	418.3 ± 4.4	0.64 ± 0.48	14.9 ± 2.8	76.6 ± 13.7
Other data in the measurement period (April to October)	2.07 ± 1.72	551.1 ± 403.7	403.3 ± 21.6	1.33 ± 1.18	20.1 ± 7.2	57.8 ± 22.4

increase starting from 6 October. High levels of BC and CO exceeding 1000 ppbv and 10 μg m^{-3}, respectively were maintained until 10 October. A summary of BC, CO, CO_2, and meteorological conditions observed at Miyun during the episode period is presented in Table 3. During this period, the lowest concentrations of BC, CO, and CO_2 exceeded their corresponding 95th percentile of all other data from April to October 2010. The 48 h back trajectories for the episode period (Figure 7), calculated by the Hybrid Single-Particle Lagrangian Integrated Trajectory (HYSPLIT) model (version 4.9) [*Draxier and Hess*, 1998], suggest that air masses were transported through the south of Beijing and likely originated from central east China. Given the relatively long duration of the episode and air mass trajectories, this high pollution period was influenced not only by emissions from the Beijing urban area but also from regional emissions in the NCP region, such as the Hebei and Henan provinces. This is consistent with NASA's satellite observations of aerosol optical depths during this period, which indicated that the pollution episode was a more regional-scale pollution event extending southward and northward from Beijing to east and central China (http://earthobservatory.nasa.gov/IOTD/view.php?id = 46375&src = eoa-iotd; accessed 15 December 2010). The stagnant meteorological conditions during the episode (Table 3), including weak wind, higher temperature, and smaller relative humidity, were favorable for the buildup of regional pollutions.

4. Discussion

4.1. Correlation Between BC and Other Species

[13] Many types of trace gases are emitted from the same combustion processes that emit BC, including CO, CO_2, SO_2, and NO_x. The emission ratio between BC and these trace gases differs by combustion type and condition [*Han et al.*, 2009; *Kondo et al.*, 2006], as indicated in Table 4, which summarizes the ratio between the emission factors of BC to other species (CO, CO_2, and NO_x) by sector and fuel type. To make a direct comparison of the ratio of emission factors with the observed concentration ratios, the units of the emission factor ratios have been converted to μg m^{-3}/ppbv (for BC/CO and BC/NO_x) or μg m^{-3}/ppmv (for BC/CO_2) using the ideal gas law. We adopted a uniform temperature and pressure of 273.15 K and 1013 hPa, respectively, in unit conversion. Sources of BC that are colocated with those of the trace gases will result in correlations in their concentration variations because their variances are affected by the same atmospheric transport. Therefore, additional constraints on emissions can be provided from the relationship between BC and the trace gases observed concurrently at the Miyun site than from BC observations alone.

[14] The correlation coefficients of BC-CO, BC-CO_2, BC-NO_y, and BC-SO_2 observed in the daytime at the site are summarized in Table 5. Concentrations of BC are positively correlated with CO, CO_2, and NO_y in the spring. The correlations become much lower in the summer for the following reasons. First, CO_2 is not a good indicator of combustion in the summer because its variability is dominated by exchanges with the biosphere. Second, concentrations of NO_y are strongly affected by more active chemical reactions in the summer than by emissions. Third, wet deposition of BC is enhanced in the summer as a result of increasing precipitation. The correlation of BC with SO_2 is weaker than that with CO or NO_y in all seasons, suggesting that coal may not be a big source of BC at Miyun compared with other types of emissions such as biofuel.

[15] The ΔBC/ΔCO, ΔBC/ΔCO_2 (excluding summer), and ΔBC/ΔNO_y ratios were 0.0046 ± 0.0001 μg m^{-3}/ppbv, 0.208 ± 0.0056 μg m^{-3}/ppmv, and 0.192 ± 0.004 μg m^{-3}/ppbv, respectively, during the study period. These enhancement ratios were derived from the correlation slopes of the reduced-major-axis regression that treats the two variables as symmetrical [*Hirsch and Gilroy*, 1984]. The seasonal and diurnal variability of the BC to trace gas ratios is summarized in Figure 8. The ratios are generally higher at night. Residential cooking peaks from 5 to 8 P.M. in the countryside, causing the ratio to increase at night as the local residential sources tend to have higher BC emissions relative to trace gases [*Streets et al.*, 2003a]. The higher ΔBC/ΔNO_y in the summer is a result of enhanced crop residue burning in June,

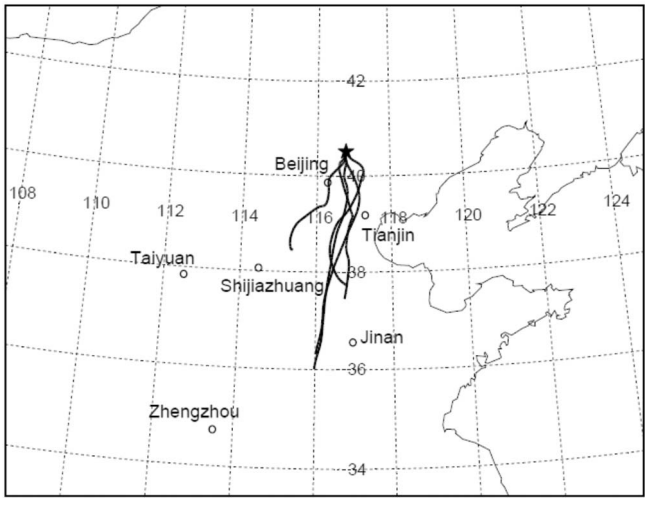


Figure 7. The 48 h back trajectories for observations from 6 to 10 October. Locations of big cities are shown on the map.

Table 4. The BC/CO, BC/CO_2, and BC/NO_x Emission Ratios Calculated Using the Published Emission Factors in China

	Industry[a]		Vehicles[a,b,c]		Residential[a]		Open Biomass Burning[d]
	Coal	Oil	Gasoline	Diesel	Coal	Biofuel	
BC/CO[e] (μg m^{-3}/ppbv)	0.0019–0.0200	—	0.0002–0.0008	0.0140–0.0388	0.0020–0.0625	0.0162–0.0291	0.0056–0.0133
BC/CO_2[f] (μg m^{-3}/ppmv)	0.0438–0.8061	0.1576–0.2349	0.0483–0.2597	0.7852–2.1745	0.1162–3.8886	1.5322–1.9296	0.5845–0.8946
BC/NO_x[g] (μg m^{-3}/ppbv)	0.0178–0.5177	0.0707–0.2207	0.0059–0.0316	0.0424–0.1138	0.1100–6.3845	2.6093–3.8030	0.2528–0.8855

[a] *Streets et al.* [2003b].
[b] *Bond et al.* [2004].
[c] *Zhang et al.* [2009].
[d] *Andreae and Merlet* [2001].
[e] The value 1 μg m^{-3}/ppbv = 1.25 g/g.
[f] The value 1 μg m^{-3}/ppbm = 1964.29 g/g.
[g] The value 1 μg m^{-3}/ppbv = 2.05g/g.

as discussed previously. Crop residue burning is a large emitter of BC but not a significant source of NO_y because of the lower combustion temperature and relatively high moisture content of the material burned. Because of the limited data coverage of NO_y and the high impact of the biosphere on CO_2, we mainly focus on the correlation of BC to CO in later discussions.

[16] Table 6 summarizes the ΔBC/ΔCO ratio measured in China by previous studies. The units in the table were all converted to μg m^{-3}/ppbv for comparison. Only the work of *Li et al.* [2007] and this study used the method of light absorption to measure BC, while the thermal-optical transmittance method, which measures elemental carbon, (EC) was used in other studies. The ΔBC/ΔCO measured in this study is comparable to observations at another rural site near Beijing-Changping. Summertime observations at our site and the Changping site [*Zhou et al.*, 2009], representing the outflow of the Beijing urban area, indicate a ΔBC/ΔCO ratio of about 0.004 μg m^{-3}/ppbv. This is slightly less than the ratio of 0.0048 μg m^{-3}/ppbv observed in the Beijing urban area by *Han et al.* [2009]. Measurements at another rural measurement located to the southeast of Beijing, Xianghe [*Li et al.*, 2007], indicated a ΔBC/ΔCO of 0.0064 μg m^{-3}/ppbv in spring, which is higher than that in this study. This is because the Xianghe site samples primarily the polluted urban outflow from Beijing in the spring. Although the observations in Table 6 indicate large differences of up to a factor of 2 in observed ΔBC/ΔCO ratios among three big Chinese cities (Beijing, Shanghai, and Guangzhou), the annual-mean BC/CO emission ratios derived from the bottom-up inventory of *Zhang et al.* [2009] (see Figure 1b) do not show such large differences between them, ranging from 0.0083 μg m^{-3}/ppbv in Guangzhou to 0.0102 μg m^{-3}/ppbv in Shanghai. The discrepancy may be due to a different spatial and temporal window used in the observation and emission inventory (e.g., observation ratio in one season versus annual-mean emission ratio, point-based observations versus grid-mean emissions) and atmospheric processes such as wet deposition, but a detailed comparison is needed to utilize the limited observations to constrain emission estimates. Our discussion in section 4.3 is such an attempt for the Beijing area. Continuous BC observations were made at Cape Hedo (26.9°N, 128.3°E, 60 m asl) on Okinawa Island, Japan, in the East China Sea for 2008, also using COSMOS [*Kondo et al.*, 2011b; *Verma et al.*, 2011]. After selecting the data strongly influenced by Chinese emissions, the annual-mean BC/CO ratio observed at Hedo was 0.0053 μg m^{-3}/ppbv, slightly higher than the mean ratio of 0.0046 ± 0.0001 μg m^{-3}/ppbv at Miyun between April and October 2010. The overall higher ΔBC/ΔCO ratio at Hedo may be due to the influence of higher BC/CO ratios from China during heating seasons.

4.2. Cluster Analysis

[17] To identify the transport pathways of air masses sampled at the site, we used the HYSPLIT model to calculate the back trajectories of all the observations during the study period. Back trajectories are calculated at 1200 local time everyday with an initial height of 6 m and time step of 1 h. The meteorological data used are the Global Data Assimilation System (GDAS) reanalysis data at 1° × 1° spatial resolution. The back trajectories are classified into two major air mass groups based on cluster analysis [*Dorling et al.*, 1992], as illustrated in Figure 9: Siberian (Figure 9a) and NCP (Figure 9b). The Siberian air masses mainly originate from the north, such as the eastern Siberian region, and can be regarded as the clean background air from the north. This group accounts for 29% of all the trajectories. The NCP air masses originate and travel around the NCP, including the urban areas of big cities such as Beijing and Tianjin. This group accounts for 68% of the trajectories. Only 3% of the air masses that originate from over the long distance from Siberia do not belong to the two clusters and are not shown.

[18] The percentage of contribution of each air mass group to total observations is summarized in Figure 4a by month. The NCP group is the predominant air mass group from June to September, accounting for 100% during June–July and over 70% during August–September. The Siberian group makes important contributions only in the spring and in October. The peak at around 0.11 μg m^{-3} in the frequency distribution of BC in the spring and fall (Figure 5) results from the Siberian air masses and may be taken as the mean background concentration of BC at the site. Table 7 summarizes the statistics of BC, CO, CO_2, SO_2, and NO_y for the two air mass groups. The average concentrations of BC, CO,

Table 5. Square of Correlation Coefficients (R^2) Between BC and Other Trace Gases in the Daytime (0800–1800 LT) at Miyun

	All Data	Spring	Summer	Fall
BC/CO	0.51	0.64	0.47	0.54
BC/CO_2	0.18	0.69	0.02	0.37
BC/NO_y	0.58	0.85	0.43	NA[a]
BC/SO_2	0.02	0.46	0.01	0.35

[a] The NO_y data were not available here because of the instrument failure.

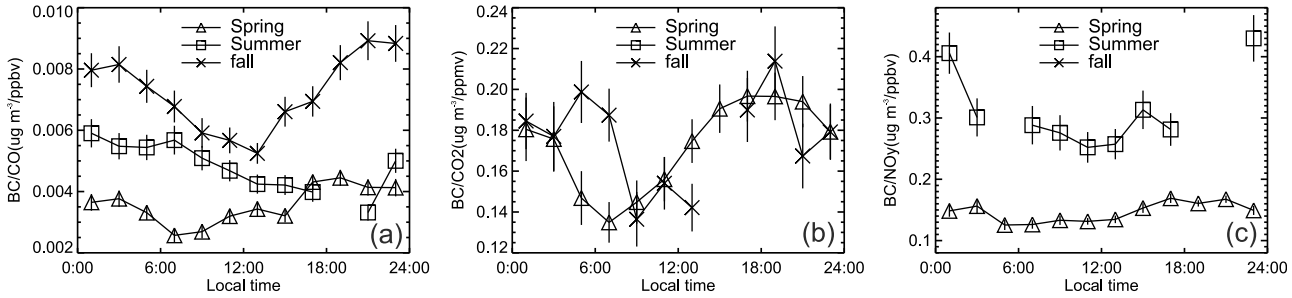


Figure 8. The diurnal variation of the observed (a) $\Delta BC/\Delta CO$, (b) $\Delta BC/\Delta CO_2$, and (c) $\Delta BC/\Delta NO_y$. The ratios were calculated every 2 h. The correlations with a R^2 of less than 0.4 were excluded, and the error bars indicate the uncertainty of the ratio. The NO_y data were not available since late July because of the instrument failure.

SO_2, and NO_y in the NCP group are all higher than in the Siberian group by about a factor of 2, supporting the different origins of the two clusters by trajectory analysis. The cluster analysis illustrates the seasonal changes in synoptic transport patterns associated with the monsoonal circulation.

[19] The monthly mean concentrations of BC and CO in the Siberian and the NCP air mass groups are shown in Figures 4a and 4b, respectively. For both species, the month-to-month variations within each cluster are much lower than the difference between the two clusters. Therefore, the relative contribution of the two clusters sampled in each month plays a large role in determining the monthly mean concentrations of BC and CO at the site. As almost all the air masses sampled in June and July are of the NCP type, the monthly mean concentrations of BC and CO in these two months are much higher than in other months. In contrast, air masses sampled in spring and October consist of a combination of Siberian and NCP types. The high levels of BC and CO in the NCP cluster in June reflected the influence of crop residue burning, while the high concentrations in October were caused by a pollution episode from 6 to 10 October.

[20] The correlations of BC to CO by cluster are plotted in Figure 10. The $\Delta BC/\Delta CO$ ratio in the NCP cluster (0.0050 ± 0.0001 $\mu g\ m^{-3}$/ppbv) is higher than that in the Siberian cluster (0.0026 ± 0.0001 $\mu g\ m^{-3}$/ppbv) by almost a factor of 2. This indicates that the source characteristics represented by the clusters are different. According to the back trajectories, air masses in the NCP cluster are strongly influenced by emission sources from the Beijing urban area and the NCP, while those in the Siberian cluster represent background flow and distant sources from the north. As CO has a longer lifetime than BC, the correlation slope of BC to CO will decrease with increasing transport time from the sources. Although the correlation is weaker in the NCP than in the Siberian cluster, reflecting the more complex source mixture and transport routes in the NCP air mass group, it is statistically significant.

4.3. Top-Down BC/CO Emission Ratio

[21] The average observed $\Delta BC/\Delta CO$ ratio of the NCP air masses will provide useful top-down constraints on the average BC/CO emission ratios for the source region from which the air masses originate. The range of the source regions for the NCP air masses is represented by the red box in Figure 9b, which includes the Beijing metropolitan area and the NCP. Over 80% of the NCP back trajectories pass through the boundary layer of the source region at least 1 day before arriving at Miyun, although the exact boundary of the source region is chosen rather arbitrarily. As the BC/CO emission ratio is distinctly different by sectors (see Table 4), the observed mean $\Delta BC/\Delta CO$ ratio will also help identify the major sources of BC from the source region.

[22] The observed ratio depends not only on emission characteristics but also on atmospheric processes that exert different influences on the two species. The processes include wet and dry depositions that affect BC but not CO, chemical reactions with OH radicals that affect CO, and mixing that affects both species; equation (1) is used to relate the BC to CO ratio observed in the atmosphere ($\Delta BC/\Delta CO|_t$) to that from emissions ($BC/CO|_{E,\ \text{top-down}}$) after an atmospheric traveling time of t. F_{wet}, F_{dry}, F_{chem}, and F_{mixing} denote the impact on the observed $\Delta BC/\Delta CO$ of wet deposition, dry deposition, chemistry, and atmospheric mixing, respectively. $\Delta BC/\Delta CO|_t$ is assumed to be a known quantity derived from the NCP air masses that are representative of regional pollution. The days of observations heavily influenced by biomass burning in June were excluded as these emissions were

Table 6. The Observed $\Delta BC/\Delta CO$ Ratio in China With Standard Error[a]

Location	BC/CO in Spring	BC/CO in Summer	BC/CO in Fall	Reference
Beijing (rural, Miyun)	0.0033 ± 0.0001	0.0045 ± 0.0002	0.0077 ± 0.0002	This study
Beijing (rural, Changping, north of Beijing city, southwest of Miyun)	—	0.0042	—	*Zhou et al.* [2009]
Hebei (rural, Xianghe, southeast of Beijing city)	0.0064	—	—	*Li et al.* [2007]
Beijing (urban)	0.0034	0.0048	0.0058	*Han et al.* [2009]
Shanghai (urban)	0.0115	—	—	*Zhou et al.* [2009]
Guangzhou (urban)	—	0.0054 ± 0.0004	—	*Verma et al.* [2010]
Guangzhou (urban)	—	—	0.0079	*Andreae et al.* [2008]

[a]Units are $\mu g\ m^{-3}$/ppbv.

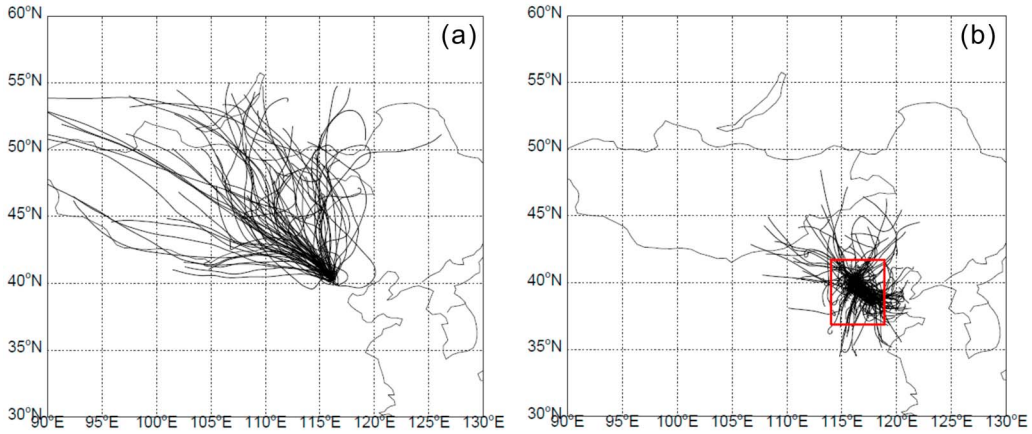


Figure 9. The 48 h back trajectories of (a) the Siberian and (b) the NCP air masses from April to October 2010. The region of NCP has been encircled by red lines in Figure 9b.

not reflected in the inventory. We use $BC/CO|_{E,\ top\text{-}down}$ to denote the BC to CO ratio of composite emissions from Beijing and the NCP, where the NCP air masses originate. As $BC/CO|_{E,\ top\text{-}down}$ is derived from the observed atmospheric concentration ratio ($\Delta BC/\Delta CO|_t$), it is referred to as the top-down BC/CO emission ratio and will be compared with the emission ratio from bottom-up emission inventories (bottom-up emission ratio, $BC/CO|_{E,\ bottom\text{-}up}$) in the next session. The purpose of this section is to estimate the average $BC/CO|_{E,\ top\text{-}down}$ for the source region identified above from $\Delta BC/\Delta CO|_t$ on the basis of screening and/or quantitative estimate of F_{wet}, F_{dry}, F_{chem}, and F_{mixing}:

$$\Delta BC/\Delta CO|_t = BC/CO|_{E,\ top-down} F_{dry} F_{chem} F_{mixing} F_{wet}. \quad (1)$$

[23] As wet deposition will reduce the $\Delta BC/\Delta CO$ ratios in the atmosphere, we first excluded the influence of wet deposition on the observations. The merged high-quality (HQ)-infrared (IR) precipitation data observed by the Tropical Rainfall Measuring Mission (TRMM) satellite instrument [*Huffman et al.*, 2001] is adopted for wet deposition screening. The TRMM precipitation data have a temporal resolution of 3 h and a horizontal resolution of 0.25° × 0.25° extending from 50°S to 50°N. Previous studies have found good correlations between TRMM results and ground measurements ($R^2 = 0.3$–0.9), with relative errors of less than 20% [*Liao et al.*, 2001; *Wang and David*, 2010]. We calculated the accumulative precipitation along the back trajectories of the NCP air masses during the last 48 h to identify the BC-CO data pairs that have been influenced by wet deposition. Figure 11 illustrates the change in the $\Delta BC/\Delta CO$ ratio observed at Miyun for different intervals of accumulated precipitation of the NCP cluster in the daytime. The $\Delta BC/\Delta CO$ ratio of air masses receiving less than 2 mm precipitation during the last 48 h is more than double that of air masses receiving higher levels of precipitation. In light of Figure 11, we removed the BC-CO data pairs that were influenced by more than 2 mm accumulative precipitation along their back trajectories during the last 48 h so as to minimize the impact of wet deposition while retaining a sufficient number of data points for statistical significance. Figure 12 presents two sample trajectories overlaid with TRMM precipitation to illustrate the process of wet deposition screening. The back trajectory for 1 July (Figure 12a) did not receive precipitation greater than 2 mm, so the BC-CO observation pairs on 1 July were used. In contrast, heavy precipitation was found along the back trajectory for 1 August (Figure 12b), so the observations on 1 August were discarded in the correlation analysis. *Matsui et al.* [2011] adopted a similar approach in analyzing the impact of wet removal on BC measured during the ARCTAS aircraft campaign, and the precipitation threshold used in their study was 5 mm. After the wet deposition screening, a total of 194 BC-CO data pairs, accounting for 26% of the NCP air mass group, was left, and the $\Delta BC/\Delta CO$ ratio for them (denoted as $\Delta BC/\Delta CO|_{t,\ no\text{-}wet}$) is 0.0084 ± 0.0004 $\mu g\ m^{-3}$/ppbv (Figure 10c). $\Delta BC/\Delta CO|_{t,\ no\text{-}wet}$ is 68% larger than $\Delta BC/\Delta CO|_t$ (0.005 $\mu g\ m^{-3}$/ppbv), the original slope prior to precipitation screening, illustrating again the large impact of wet deposition on the observed $\Delta BC/\Delta CO$ ratio. To estimate the uncertainty in the process of precipitation screening, we conducted two sensitivity calculations in which the precipitation-screening thresholds were chosen as 1 and 3 mm, respectively. $\Delta BC/\Delta CO|_{t,\ no\text{-}wet}$ derived from the sensitivity calculations was different by ±19% from the value derived using the 2 mm precipitation-screening threshold. Therefore, we estimated the uncertainty of $\Delta BC/\Delta CO|_{t,\ no\text{-}wet}$ to be 19%.

Table 7. Trace Species Concentrations for the Two Different Clusters in the Daytime (0800–1800 LT) at Miyun

	Measurement	BC ($\mu g\ m^{-3}$)	SO_2 (ppb)	CO (ppb)	CO_2 (ppm)	NO_y (ppb)
Siberian Cluster	mean ± standard deviation	0.64 ± 0.72	2.64 ± 5.11	266.5 ± 297.9	395.4 ± 20.3	8.08 ± 6.83
	median	0.36	0.74	151.6	397.4	6.12
NCP Cluster	mean ± standard deviation	2.72 ± 2.31	4.89 ± 5.36	677.9 ± 385.5	400.2 ± 19.3	17.09 ± 7.97
	median	2.09	2.62	593.6	401.1	15.70

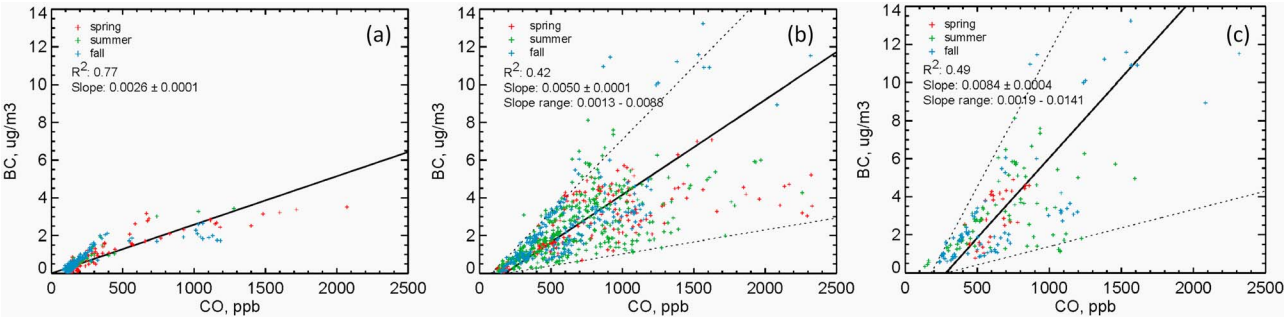


Figure 10. The relationship between BC and CO in (a) the Siberian air mass group, (b) the NCP air mass group, and (c) the NCP air masses after excluding the wet deposition influence. Different colors represent different seasons. The unit of the slope is μg m^{-3}/ppbv.

After the wet deposition screening, we assume that the F_{wet} term in equation 1 can be neglected (i.e., $F_{\mathrm{wet}} = 1$), and equation (1) becomes

$$\Delta\mathrm{BC}/\Delta\mathrm{CO}\big|_{t,\ \mathrm{no-wet}} = \mathrm{BC}/\mathrm{CO}\big|_{E,\ \mathrm{top-down}} F_{\mathrm{dry}} F_{chem} F_{\mathrm{mixing}}. \quad (2)$$

[24] Vertical mixing and convection are major atmospheric mixing processes affecting near-source surface observations. The exclusion of wet deposition discussed above is expected to exclude also the impact of atmospheric mixing during convective and large-scale precipitation on the observations. As the dry deposition of BC and chemical reaction of CO occur on much longer time scales (~days) compared with boundary layer mixing and convection (~hours), we can neglect the coupling between mixing and dry deposition (for BC) or chemistry (for CO). We argue therefore that mixing by itself, absent of deposition or chemistry, will affect BC and CO indifferently and thus not alter the ΔBC/ΔCO ratio. Therefore, with the wet deposition screening, F_{mixing} can be taken to be 1 and equation (2) reduces to

$$\Delta\mathrm{BC}/\Delta\mathrm{CO}\big|_{t,\ \mathrm{no-wet}} = \mathrm{BC}/\mathrm{CO}\big|_{E,\ \mathrm{top-down}} F_{\mathrm{dry}} F_{\mathrm{chem}}. \quad (3)$$

[25] As F_{dry} and F_{chem} are independent of each other, they can be estimated using the different lifetimes of the two species:

$$\Delta\mathrm{BC}/\Delta\mathrm{CO}\big|_{t,\ \mathrm{no-wet}} = \mathrm{BC}/\mathrm{CO}\big|_{E,\ \mathrm{top-down}} \exp(t/\tau_{\mathrm{BC}} - t/\tau_{\mathrm{CO}}), \quad (4)$$

where τ_{BC} and τ_{CO} (in units of days) denote the lifetimes of BC (without wet deposition) and CO in the atmosphere, respectively. We further define

$$F_{\mathrm{dry+chem}} = \exp(t/\tau_{\mathrm{BC}} - t/\tau_{\mathrm{CO}}). \quad (5)$$

Rearrangement of equation (4) and replacement by equation (5) give

$$\mathrm{BC}/\mathrm{CO}\big|_{E,\ \mathrm{top-down}} = \Delta\mathrm{BC}/\Delta\mathrm{CO}\big|_{t,\ \mathrm{no-wet}} / F_{\mathrm{dry+chem}}. \quad (6)$$

[26] Although τ_{BC}, τ_{CO}, and t depend on many factors, a probable range can be given for each parameter. The review paper by *Koch et al.* [2009] estimated the lifetime of BC (τ_{BC}) to have a range of 4.9–11.4 days based on the simulation results from a number of atmospheric chemical transport models. The impact of wet removal on τ_{BC} is included in these models [*Koch et al.*, 2009]. As we have excluded the observations influenced by wet deposition, we tentatively choose an arbitrarily narrower range of 8–11.4 days for τ_{BC} than that by *Koch et al.* [2009]. The lifetime of CO (τ_{CO}) is estimated to range from 30 to 90 days during the measurement period [*Khalil and Rasmussen*, 1994, 1990; *Novelli et al.*, 1998]. Considering the average wind speeds and back trajectory analysis (Figure 9b), we assume t to be less than 2 days for the NCP air masses traveling around the NCP region. As τ_{CO} is almost an order of magnitude larger than τ_{BC}, it has a much smaller influence on $F_{\mathrm{dry+chem.}}$ than τ_{BC}. When τ_{CO} is set to be 30 days, the change of $F_{\mathrm{dry+chem.}}$ with different t and τ_{BC} is shown in Figure 13. According to the range of the three parameters, $F_{\mathrm{dry+chem}}$ ranges from 0.79 to 1 with a mean of 0.88. This suggests that the process of treating $F_{\mathrm{dry+chem.}}$ has an uncertainty of about 10%.

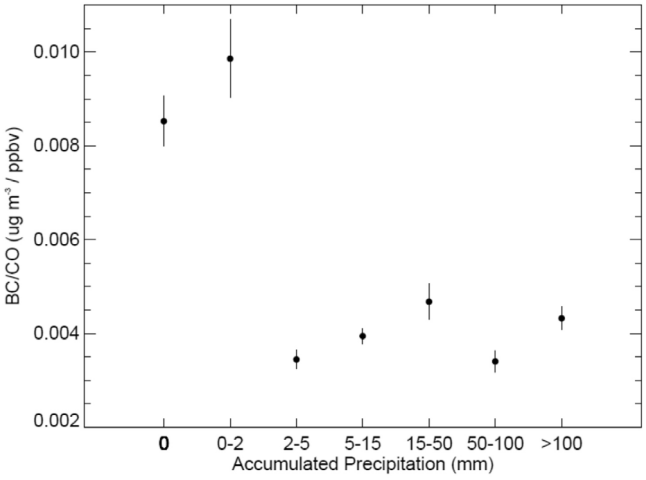


Figure 11. The observed ΔBC/ΔCO ratio in the NCP air mass group separated by different accumulated precipitations along the individual trajectories. The percentage of BC-CO pairs in each interval is also given above the x axis. The square of the correlation coefficient between BC and CO in each interval is larger than 0.4 except for the last interval (>100 mm), which has a R^2 of 0.3.

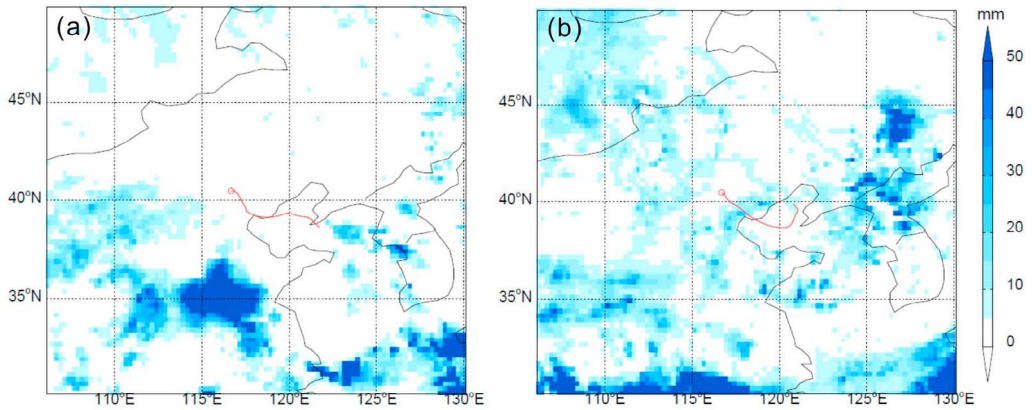


Figure 12. The distribution of 48 h accumulative precipitation from TRMM (color coded) and back trajectories (red lines) on (a) 1 July and (b) 10 July 2010.

[27] From equation (6), we estimated that the mean top-down BC/CO emission ratio ($BC/CO|_{E,\ top\text{-}down}$) is 0.0095 $\mu g\ m^{-3}$/ppbv. This is 90% higher than the observed $\Delta BC/\Delta CO$ ratio for all NCP air masses ($BC/CO|_t$), and the difference is attributed to the impact of atmospheric processes, as discussed above. The overall uncertainty of $BC/CO|_{E,\ top\text{-}down}$ is estimated to be 21% (or $\pm$ 0.002 $\mu g\ m^{-3}$/ppbv), derived as the RMS error of $\Delta BC/\Delta CO|_{t,\ no\text{-}wet}$ (19%) and $F_{dry+chem}$ (10%).

4.4. Emission Evaluation

[28] In this section we compare the average top-down BC/CO emission ratio derived above ($BC/CO|_{E,\ top\text{-}down}$) with the emission ratio of the two species derived from the bottom-up inventories for Beijing and the NCP ($BC/CO|_{E,\ bottom\text{-}up}$). The inventory data adopted in this study were taken from *Zhang et al.* [2009], who reported Chinese emissions for 2006 at a spatial resolution of 0.5° × 0.5°. Compared with the global BC inventory for 2000 by *Bond et al.* [2004], the inventory of *Zhang et al.* [2009] adopted updated activity data specific 2006 while using similar emission factors. The annual total of BC emissions from China is 1.81 Tg for 2006 [*Zhang et al.*, 2009], compared with that of 1.36 Tg for 2000 reported by *Bond et al.* [2004]. According to the inventory of *Zhang et al.* [2009], major sources of BC in Beijing are residential combustion and industrial processes, which contribute to 54% and 30% of the annual total emissions, respectively. As emissions of both CO and BC exhibit large seasonality introduced by residential heating, the month-to-month scaling factors provided by *Zhang et al.* [2009] are applied to the annual total emissions to obtain the amount of emissions during the observation (April–October). The emissions of BC and CO and their ratios from different sectors in Beijing and the NCP are summarized in Table 8.

[29] As shown in Table 8, the composite bottom-up BC/CO emission ratios in Beijing (0.0116 $\mu g\ m^{-3}$/ppbv) and the NCP (0.0121 $\mu g\ m^{-3}$/ppbv) are 18% and 21% higher, respectively, than the top-down emission ratio (0.0095 $\mu g\ m^{-3}$/ppbv). The discrepancy is substantially smaller than the uncertainty bound of the bottom-up emission inventory for BC (±208%) and CO (±70%) [*Zhang et al.*, 2009]. Considering the uncertainties in $BC/CO|_{E,\ top\text{-}down}$ (±21%), the comparison suggests that the bottom-up inventory provides a good representation of the composite BC to CO emission ratio for Beijing and NCP that is consistent within 20% of the observed concentration ratio at Miyun. The difference is substantially lower than the uncertainty range reported for the emissions of both species. However, it is still important to examine the differences and to identify potential sources of biases in the bottom-up emission estimates that will resolve the discrepancy, pointing to possible directions for future improvements of emission estimates.

[30] The BC to CO emission ratios for individual sectors are distinctly different from each other as supported by field measurements of emission factors (i.e., Table 4 and references therein). In the following discussion we assume that the sector-by-sector difference in the BC/CO emission ratio is correct; that is, the residential sector has the highest BC/CO ratio, followed in decreasing order by the industry and transportation sector. Since the power sector emits very small amounts of BC and CO compared with other sectors (low correlation of BC-SO_2 also indicates this), it is excluded from our discussion. We further assume no significant change in combustion characteristics and thus in the overall BC to CO emission ratio in each sector from 2006 to 2010. Although some pollution control measures during the Beijing 2008 Olympic Games may have resulted in short-

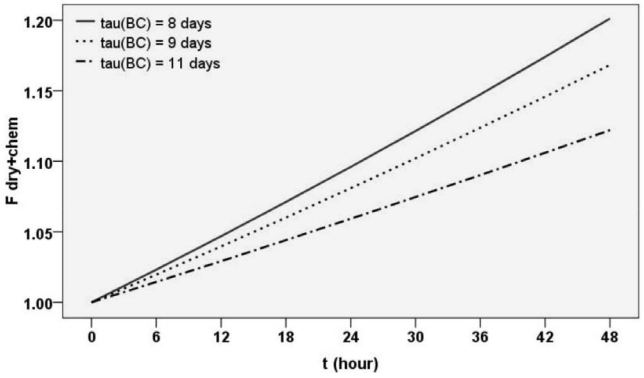


Figure 13. Changes of $F_{dry+chem.}$ with different t and τ_{BC} while τ_{CO} = 30 days.

Table 8. The Emissions of BC and CO and Their Ratios for Beijing (39°N–40.5°N; 115.5°E–117°E) and North China Plain (37°N–42.5°N; 114.5°E–120°E) Derived From the Bottom-Up Anthropogenic Emission Inventory of *Zhang et al.* [2009][a]

	Beijing			North China Plain		
Sector	BC Emission (Gg)	CO Emission (Gg)	BC/CO[b] (μg m^{-3}/ppbv)	BC Emission (Gg)	CO Emission (Gg)	BC/CO (μg m^{-3}/ppbv)
Industry	4.67 (30.36)[c]	813.33 (49.17)	0.0072	30.83 (34.42)	5087.10 (54.93)	0.0076
Power	0.21 (1.37)	14.88 (0.90)	0.0177	1.60 (1.79)	97.65 (1.05)	0.0205
Residential	8.23 (53.51)	277.51 (16.78)	0.0371	45.59 (50.91)	1959.96 (21.16)	0.0291
Transport	2.27 (14.76)	578.32 (33.15)	0.0052	11.54 (12.88)	2116.21 (22.85)	0.0068
Total	15.38	1654.05	0.0116	89.55	9290.91	0.0121
Observed ΔBC/ΔCO for NCP air masses			0.0050 ± 0.0001 (0.0013–0.0088)[d,e]			
Top-down BC/CO emission ratio			0.0095 ± 0.0004 (0.0019–0.0177)[d,e]			

[a]The top-down BC/CO ratio derived from Miyun observations is shown for comparison.
[b]Unit convention here: 1 μg m^{-3}/ppbv = 1.25 Gg/Gg.
[c]The number inside the parentheses indicates the percentage of contribution of each sector to total emissions (%).
[d]Units: μg m^{-3}/ppbv.
[e]The numbers in the parentheses refer to the range of the slopes shown in Figure 10.

term reductions and subsequent slower growth in the overall emissions of BC and CO from some sectors, we do not have evidence to anticipate major changes in combustion or fuel types within each sector that might cause the BC to CO emission ratio to be significantly different after 2008.

[31] As shown in Table 8, the residential sector has the highest BC to CO ratio (0.0371 μg m^{-3}/ppbv in Beijing and 0.0291 μg m^{-3}/ppbv in the NCP), and it is the only sector (except for power) with a BC/CO emission ratio exceeding $BC/CO|_{E,\ top\text{-}down}$ by about a factor of 2. The residential sector has a BC/CO ratio exceeding also the upper range of the BC/CO ratio derived from ambient measurements by a factor of 2. In contrast, the BC/CO emission ratio from the industry and transportation sector is very close to $BC/CO|_{E,\ top\text{-}down}$. This suggests that the industry and transportation sectors are most likely the dominant sources of BC from Beijing and the NCP rather than the residential sector, as suggested by the bottom-up inventory, or that the BC/CO emission ratio from this sector is highly overestimated. Emissions from the residential sector are also uncertain, as accurate information on the activity level is very hard to obtain compared with that of other sectors [*Bond et al.*, 2004]. Therefore, in order to yield a lower composite BC to CO emission ratio, the most sensible scenario is that the residential sector has lower activity levels while maintaining the same BC/CO ratio or a lower BC/CO emission ratio. When emissions from other sectors remain unchanged, we identify three possibilities of emission adjustment from the residential sector: (1) both BC and CO emissions from the residential sector are reduced by 46% while keeping the same BC to CO emission ratio; or (2) the BC emission factor from the residential sector is reduced by 34% with no change for CO, reducing the BC/CO emission ratio from the residential sector to 0.024 μg m^{-3}/ppbv in Beijing; or (3) the CO emission factor from the residential sector is increased by 133% with no change for BC, reducing the BC/CO emission ratio from the sector to about 0.016 μg m^{-3}/ppbv in Beijing. The three cases point to different directions for the emission change from the residential sector and the quantitative adjustment in each case all lie within the uncertainty bound of bottom-up emissions for both BC and CO.

[32] The industry and transportation sectors have smaller BC/CO emission ratios than $BC/CO|_{E,\ top\text{-}down}$, so increasing the activity levels of these two sectors will also bring $BC/CO|_{E,\ bottom\text{-}up}$ closer to $BC/CO|_{E,\ top\text{-}down}$. We do not consider reducing the BC/CO ratios from the two sectors because they are close to $BC/CO|_{E,\ top\text{-}down}$. If the activity level from the residential sector is unchanged, emissions of both BC and CO from the industry and transportation sectors would need to be doubled in order to make $BC/CO|_{E,\ bottom\text{-}up}$ equal to $BC/CO|_{E,\ top\text{-}down}$. As the sector's activity level is constrained by the overall vehicle miles traveled for the transportation sector and by industrial outputs for the industry sector that are constrained by national statistics, it would be difficult to account for a change of 100% in the activity levels for these sectors. Therefore, even if the activity levels from the industry and transportation sectors are underestimated, emissions from the residential sector would still require adjustment, but by less than that indicated above.

[33] Although this study cannot give definite estimates of BC or CO emissions from the source region because of the large degree of freedom in determining the average BC/CO emission ratios, it identifies, using atmospheric observations independent of the bottom-up inventory, major source types of BC for the source region and the residential sector as the source of discrepancy and the area in need of improvements. Future analysis will be necessary that combines a higher-resolution transport model and detailed inventories of all BC and CO sources to simulate the BC and CO concentrations and their correlations at Miyun in order to quantitatively evaluate the biases of each species' emissions.

[34] Previous studies have evaluated emission inventories of BC in China using measurement data or model simulation. Some studies reported that the Chinese BC inventories have a bias of less than 25% [*Verma et al.*, 2010; *Carmichael et al.*, 2003; *Han et al.*, 2009]. The top-down estimate of China's BC emissions by *Kondo et al.* [2011b], derived from continuous BC measurements at a remote site (Cape Hedo) in the East China Sea in combination with a chemical transport model, was 1.92 Tg/yr, very close to the value estimated by *Zhang et al.* [2009]. However, *Tan et al.* [2004] indicate that Chinese emissions of BC were highly underestimated. Many researchers have pointed to the problem that the emissions or emission factors from the residential sector may be overestimated in China [*Verma et al.*, 2010; *Han et al.*, 2009; *Chen et al.*, 2005; *Zhi et al.*, 2008]. This is consistent with our

conclusion that BC emissions from the residential sector are likely overestimated for Beijing and the NCP region relative to CO emissions.

5. Concluding Remarks

[35] BC and other important trace gases (CO, CO_2, NO_y, and SO_2) were measured from April to October in 2010 at Miyun, a rural site about 100 km northeast of the Beijing urban area. During the measurement period, the average concentration of BC was 2.26 μg m^{-3} (a standard deviation of 2.33 μg m^{-3}), lower than those reported previously for urban areas in China. BC shows moderate to strong positive correlations with CO, NO_y, and CO_2 (nonsummer), but not with SO_2, suggesting that coal may not be a big source of BC at Miyun compared with other types of emissions such as biofuel. After excluding the effect of biomass burning, the mean $\Delta BC/\Delta CO$, $\Delta BC/\Delta CO_2$ (excluding summer), and $\Delta BC/\Delta NO_y$ slopes over the study period are about 0.0046 μg m^{-3}/ppbv, 0.20 μg m^{-3}/ppmv, and 0.19 μg m^{-3}/ppbv, respectively.

[36] Two major air mass groups were identified at the site based on the back trajectory analysis: the Siberian cluster with low concentrations of BC and trace gases originating from eastern Siberia, which can be seen as the continental background air mass; and the NCP cluster with high pollutant concentrations, which mainly reflects the regional pollution of Beijing and the NCP. The NCP cluster is the predominant air mass group from June to September. The $\Delta BC/\Delta CO$ ratio in the NCP air mass group (0.0050 ± 0.0001 μg m^{-3}/ppbv) is almost twice as high as that in the Siberian cluster (0.0026 ± 0.0001 μg m^{-3}/ppbv). The source region for the NCP air masses is estimated to include the Beijing metropolitan area and the NCP.

[37] After excluding the observations influenced by wet deposition using the TRMM precipitation data, the $\Delta BC/\Delta CO$ ratio in the NCP air mass group increases by 68% to 0.0084 ± 0.0004 μg m^{-3}/ppbv, indicating the large impact of wet deposition on the observed $\Delta BC/\Delta CO$ ratio. Accounting further for the influence of dry deposition and chemistry on the observed $\Delta BC/\Delta CO$ ratio, we derived a top-down BC/CO emission ratio of 0.0095 ± 0.002 μg m^{-3}/ppbv, which is about 18% and 21% lower than the composite bottom-up BC/CO emission ratio in Beijing (0.0116 μg m^{-3}/ppbv) and the NCP (0.0121 μg m^{-3}/ppbv) suggested by the bottom-up inventory of *Zhang et al.* [2009]. The discrepancy is substantially smaller than the uncertainty bound of the bottom-up emission inventory for BC (±208%) and CO (±70%) [*Zhang et al.*, 2009], suggesting that the bottom-up inventory provides a good representation of the composite BC to CO emission ratio for Beijing and the NCP that is consistent within 20% of the observed concentration ratio at Miyun.

[38] Analysis of the BC to CO emission ratios by sector suggests that the residential sector is the only sector (excluding the power sector) with a BC/CO emission ratio exceeding the top-down constraints by more than a factor of 2, while the BC/CO emission ratios from the industry and transportation sectors are very close to $BC/CO|_{E,\text{ top-down}}$. This suggests that the industry and transportation sectors are most likely the dominant sources of BC from Beijing and the NCP rather than the residential sector as suggested by the bottom-up inventory. We showed that the difference between the mean bottom-up and top-down emission ratios was most likely to be attributed to emissions from the residential sector, which needs to have a lower share in the total emissions of BC or a much lower BC/CO emission ratio. Future analysis will be necessary that combines a higher-resolution transport model and detailed inventories of all BC and CO sources to simulate the BC and CO concentrations and their correlations at Miyun in order to quantitatively evaluate the biases of each species' emissions.

[39] **Acknowledgments.** This research was supported by the International Science and Technology Cooperation Program of China (2010DFA21300). Y. Wang acknowledges additional funding from the National Science Foundation of China (grant 41005060). This work was also supported by the Ministry of Education, Culture, Sports, Science, and Technology (MEXT), the strategic international cooperative program of the Japan Science and Technology Agency (JST), and the global environment research fund of the Japanese Ministry of the Environment (A-1101). Trace gas measurements at the Miyun site were supported by the Harvard University Center for the Environment, Harvard Smeltzer Fund, and an anonymous private foundation, and data analyses were supported in part by a National Science Foundation grant ATM-0635548. TRMM precipitation data used in this effort were acquired as part of the activities of NASA's Science Mission Directorate and are archived and distributed by the Goddard Earth Sciences (GES) Data and Information Services Center (DISC).

References

Andreae, M. O., and P. Merlet (2001), Emissions of trace gases and aerosols from biomass burning, *Global Biogeochem. Cycles*, *15*, 955–966, doi:10.1029/2000GB001382.

Andreae, M. O., O. Schmid, H. Yang, D. Chand, J. Z. Yu, L. M. Zeng, and Y. H. Zhang (2008), Optical properties and chemical composition of the atmospheric aerosol in urban Guangzhou, China, *Atmos. Environ.*, *42*(25), 6335–6350, doi:10.1016/j.atmosenv.2008.01.030.

Bergin, M. H., et al. (2001), Aerosol radiative, physical, and chemical properties in Beijing during June 1999, *J. Geophys. Res.*, *106*(D16), 17,969–17,980, doi:10.1029/2001JD900073.

Bond, T. C., D. G. Streets, K. F. Yarber, S. M. Nelson, J. H. Woo, and Z. Klimont (2004), A technology-based global inventory of black and organic carbon emissions from combustion, *J. Geophys. Res.*, *109*, D14203, doi:10.1029/2003JD003697.

Cao, G. L., X. Y. Zhang, and F. C. Zheng (2006), Inventory of black carbon and organic carbon emissions from China, *Atmos. Environ.*, *40*(34), 6516–6527, doi:10.1016/j.atmosenv.2006.05.070.

Cao, J. J., C. S. Zhu, J. C. Chow, J. G. Watson, Y. M. Han, G. H. Wang, Z. X. Shen, and Z. S. An (2009), Black carbon relationships with emissions and meteorology in Xi'an, China, *Atmos. Res.*, *94*(2), 194–202, doi:10.1016/j.atmosres.2009.05.009.

Carmichael, G. R., et al. (2003), Evaluating regional emission estimates using the TRACE-P observations, *J. Geophys. Res.*, *108*(D21), 8810, doi:10.1029/2002JD003116.

Chen, Y. J., G. Y. Sheng, X. H. Bi, Y. L. Feng, B. X. Mai, and J. M. Fu (2005), Emission factors for carbonaceous particles and polycyclic aromatic hydrocarbons from residential coal combustion in China, *Environ. Sci. Technol.*, *39*(6), 1861–1867, doi:10.1021/es0493650.

Cheng, Y., S. C. Lee, K. F. Ho, Y. Q. Wang, J. J. Cao, J. C. Chow, and J. G. Watson (2006), Black carbon measurement in a coastal area of south China, *J. Geophys. Res.*, *111*, D12310, doi:10.1029/2005JD006663.

Cooke, W. F., C. Liousse, H. Cachier, and J. Feichter (1999), Construction of a 1° × 1° fossil fuel emission data set for carbonaceous aerosol and implementation and radiative impact in the ECHAM4 model, *J. Geophys. Res.*, *104*(D18), 22,137–22,162, doi:10.1029/1999JD900187.

Cooke, W. F., V. Ramaswamy, and P. Kasibhatla (2002), A general circulation model study of the global carbonaceous aerosol distribution, *J. Geophys. Res.*, *107*(D16), 4279, doi:10.1029/2001JD001274.

Dachs, J., and S. J. Eisenreich (2000), Adsorption onto aerosol soot carbon dominates gas-particle partitioning of polycyclic aromatic hydrocarbons, *Environ. Sci. Technol.*, *34*(17), 3690–3697, doi:10.1021/es991201+.

Dan, M., G. S. Zhuang, X. X. Li, H. R. Tao, and Y. H. Zhuang (2004), The characteristics of carbonaceous species and their sources in PM2.5 in Beijing, *Atmos. Environ.*, *38*(21), 3443–3452, doi:10.1016/j.atmosenv.2004.02.052.

Dorling, S. R., T. D. Davies, and C. E. Pierce (1992), Cluster analysis: A technique for estimating the synoptic meteorological controls on air and precipitation chemistry–Method and applications, *Atmos. Environ. Part A*, *26*(14), 2575–2581, doi: 10.1016/0960-1686(92)90110-7.

Draxier, R. R., and G. D. Hess (1998), An overview of the HYSPLIT_4 modelling system for trajectories, dispersion and deposition, *Aust. Meteorol. Mag.*, *47*(4), 295–308.

Han, S., et al. (2009), Temporal variations of elemental carbon in Beijing, *J. Geophys. Res.*, *114*, D23202, doi:10.1029/2009JD012027.

He, Z., Y. J. Kim, K. O. Ogunjobi, J. E. Kim, and S. Y. Ryu (2004), Carbonaceous aerosol characteristics of PM2.5 particles in northeastern Asia in summer 2002, *Atmos. Environ.*, *38*(12), 1795–1800, doi:10.1016/j.atmosenv.2003.12.023.

Hirsch, R. M., and E. J. Gilroy (1984), Methods of fitting a straight-line to data– Examples in water resources, *Water Resour. Bull.*, *20*(5), 705–711.

Huffman, G. J., R. F. Adler, M. Morrissey, D. T. Bolvin, S. Curtis, R. Joyce, B. McGavock, and J. Susskind (2001), Global precipitation at one-degree daily resolution from multisatellite observations, *J. Hydrometeorol.*, *2*(1), 36–50, doi:10.1175/1525-7541(2001)002<0036:GPAODD>2.0.CO;2.

Jacobson, M. Z. (2001), Strong radiative heating due to the mixing state of black carbon in atmospheric aerosols, *Nature*, *409*(6821), 695–697, doi:10.1038/35055518.

Jia, Y., K. A. Rahn, K. He, T. Wen, and Y. Wang (2008), A novel technique for quantifying the regional component of urban aerosol solely from its sawtooth cycles, *J. Geophys. Res.*, *113*, D21309, doi:10.1029/2008JD010389.

Khalil, M. A. K., and R. A. Rasmussen (1990), The global cycle of carbon monoxide: Trends and mass balance, *Chemosphere*, *20*(1–2), 227–242, doi:10/1016/0045-6535(90)90098-E.

Khalil, M. A. K., and R. A. Rasmussen (1994), Global decrease in atmospheric carbon monoxide concentration, *Nature*, *370*(6491), 639–641, doi:10.1038/370639a0.

Koch, D., et al. (2009), Evaluation of black carbon estimations in global aerosol models, *Atmos. Chem. Phys.*, *9*(22), 9001–9026, doi:10.5194/acp-9-9001-2009.

Kondo, Y., et al. (2006), Temporal variations of elemental carbon in Tokyo, *J. Geophys. Res.*, *111*, D12205, doi:10.1029/2005JD006257.

Kondo, Y., et al. (2009), Stabilization of the mass absorption cross section of black carbon for filter-based absorption photometry by the use of a heated inlet, *Aerosol Sci. Technol.*, *43*(8), 741–756, doi:10.1080/02786820902889879.

Kondo, Y., L. Sahu, N. Moteki, F. Khan, N. Takegawa, X. Liu, M. Koike, and T. Miyakawa (2011a), Consistency and traceability of black carbon measurements made by laser-induced incandescence, thermal-optical transmittance, and filter-based photo-absorption techniques, *Aerosol Sci. Technol.*, *45*, 295–312, doi:10.1080/02786826.2010.533215.

Kondo, Y., N. Oshima, M. Kajino, R. Mikami, N. Moteki, N. Takegawa, R. L. Verma, Y. Kajii, S. Kato, and A. Takami (2011b), Emissions of black carbon in East Asia estimated from observations at a remote site in the East China Sea, *J. Geophys. Res.*, *116*, D16201, doi:10.1029/2011JD015637.

Li, C., L. T. Marufu, R. R. Dickerson, Z. Li, T. Wen, Y. Wang, P. Wang, H. Chen, and J. W. Stehr (2007), In situ measurements of trace gases and aerosol optical properties at a rural site in northern China during East Asian Study of tropospheric aerosols: An International Regional Experiment 2005, *J. Geophys. Res.*, *112*, D22S04, doi:10.1029/2006JD007592.

Liao, L., M. Robert, and I. Toshio (2001), Comparisons of rain rate and reflectivity factor derived from the TRMM precipitation radar and the WSR-88D over the Melbourne, Florida, site, *J. Atmos. Oceanic Technol.*, *18*, 1959–1974, doi:10.1175/1520-0426(2001)018<1959:CORRAR>2.0.CO;2.

Liousse, C., J. E. Penner, C. Chuang, J. J. Walton, H. Eddleman, and H. Cachier (1996), A global three-dimensional model study of carbonaceous aerosols, *J. Geophys. Res.*, *101*(D14), 19,411–19,432, doi:10.1029/95JD03426.

Masiello, C. A. (2004), New directions in black carbon organic geochemistry, *Mar. Chem.*, *92*(1–4), 201–213, doi:10.1016/j.marchem.2004.06.043.

Matsui, H., et al. (2011), Seasonal variation of the transport of black carbon aerosol from the Asian continent to the Arctic during the ARCTAS aircraft campaign, *J. Geophys. Res.*, *116*, D05202, doi:10.1029/2010JD015067.

Miyazaki, Y., Y. Kondo, L. K. Sahu, J. Imaru, N. Fukushima, and M. Kano (2008), Performance of a newly designed continuous soot monitoring system (COSMOS), *J. Environ. Monit.*, *10*(10), 1195–1201, doi:10.1039/b806957c.

Myhre, G., F. Stordal, K. Restad, and I. S. A. Isaksen (1998), Estimation of the direct radiative forcing due to sulfate and soot aerosols, *Tellus, Ser. B*, *50*(5), 463–477, doi:10.1034/j.1600-0889.1998.t01-4-00005.x.

Novelli, P. C., K. A. Masarie, and P. M. Lang (1998), Distributions and recent changes of carbon monoxide in the lower troposphere, *J. Geophys. Res.*, *103*(D15), 19,015–19,033, doi:10.1029/98JD01366.

Penner, J. E., H. Eddleman, and T. Novakov (1993), Towards the development of a global inventory for black carbon emissions, *Atmos. Environ. Part A*, *27*(8), 1277–1295.

Ramachandran, S., and T. A. Rajesh (2007), Black carbon aerosol mass concentrations over Ahmedabad, an urban location in western India: Comparison with urban sites in Asia, Europe, Canada, and the United States, *J. Geophys. Res.*, *112*, D06211, doi:10.1029/2006JD007488.

Ramanathan, V., and G. Carmichael (2008), Global and regional climate changes due to black carbon, *Nat. Geosci.*, *1*(4), 221–227, doi:10.1038/ngeo156.

Ramanathan, V., C. Chung, D. Kim, T. Bettge, L. Buja, J. T. Kiehl, W. M. Washington, Q. Fu, D. R. Sikka, and M. Wild (2005), Atmospheric brown clouds: impacts on South Asian climate and hydrological cycle, *Proc. Natl. Acad. Sci. U. S. A.*, *102*(15), 5326–5333, doi:10.1073/pnas.0500656102.

Solomon, S., D. Qin, M. Manning, Z. Chen, M. Marquis, K. B. Averyt, M. Tignor, and H. L. Miller (Eds.) (2007), *Climate Change 2007: The Physical Science Basis: Contribution of Working Group I to the Fourth Assessment Report on the Intergovernmental Panel on Climate Change*, Cambridge Univ. Press, Cambridge, U. K.

Streets, D. G., S. Gupta, S. T. Waldhoff, M. Q. Wang, T. C. Bond, and Y. Y. Bo (2001), Black carbon emissions in China, *Atmos. Environ.*, *35*(25), 4281–4296, doi:10.1016/S1352-2310(01)00179-0.

Streets, D. G., et al. (2003a), An inventory of gaseous and primary aerosol emissions in Asia in the year 2000, *J. Geophys. Res.*, *108*(D21), 8809, doi:10.1029/2002JD003093.

Streets, D. G., K. F. Yarber, J. H. Woo, and G. R. Carmichael (2003b), Biomass burning in Asia: Annual and seasonal estimates and atmospheric emissions, *Global Biogeochem. Cycles*, *17*(4), 1099, doi:10.1029/2003GB002040.

Tan, Q., W. L. Chameides, D. Streets, T. Wang, J. Xu, M. Bergin, and J. Woo (2004), An evaluation of TRACE-P emission inventories from China using a regional model and chemical measurements, *J. Geophys. Res.*, *109*, D22305, doi:10.1029/2004JD005071.

Verma, R. L., et al. (2010), Temporal variations of black carbon in Guangzhou, China, in summer 2006, *Atmos. Chem. Phys.*, *10*(14), 6471–6485, doi:10.5194/acp-10-6471-2010.

Verma, R. L., Y. Kondo, N. Oshima, H. Matsui, K. Kita, L. K. Sahu, S. Kato, Y. Kajii, A. Takami, and T. Miyakawa (2011), Seasonal variations of the transport of black carbon and carbon monoxide from the Asian continent to the western Pacific in the boundary layer, *J. Geophys. Res.*, *116*, D21307, doi:10.1029/2011JD015830.

Wang, J., and B. W. David (2010), Evaluation of TRMM ground-validation radar-rain errors using rain gauge measurements, *J. Appl. Meteorol. Climatol.*, *49*, 310–324, doi:10.1175/2009JAMC2264.1.

Wang, Y., M. B. McElroy, J. W. Munger, J. Hao, H. Ma, C. P. Nielsen, and Y. Chen (2008), Variations of O_3 and CO in summertime at a rural site near Beijing, *Atmos. Chem. Phys.*, *8*(21), 6355–6363, doi:10.5194/acp-8-6355-2008.

Wang, Y., J. Hao, M. B. McElroy, J. W. Munger, H. Ma, D. Chen, and C. P. Nielsen (2009), Ozone air quality during the 2008 Beijing Olympics: Effectiveness of emission restrictions, *Atmos. Chem. Phys.*, *9*(14), 5237–5251, doi:10.5194/acp-9-5237-2009.

Wang, Y., J. W. Munger, S. Xu, M. B. McElroy, J. Hao, C. P. Nielsen, and H. Ma (2010), CO_2 and its correlation with CO at a rural site near Beijing: Implications for combustion efficiency in China, *Atmos. Chem. Phys.*, *10*(18), 8881–8897, doi:10.5194/acp-10-8881-2010.

Yan, P., J. Tang, J. Huang, J. T. Mao, X. J. Zhou, Q. Liu, Z. F. Wang, and H. G. Zhou (2008), The measurement of aerosol optical properties at a rural site in northern China, *Atmos. Chem. Phys.*, *8*(8), 2229–2242, doi:10.5194/acp-8-2229-2008.

Ye, B. M., X. L. Ji, H. Z. Yang, X. H. Yao, C. K. Chan, S. H. Cadle, T. Chan, and P. A. Mulawa (2003), Concentration and chemical composition of PM2.5 in Shanghai for a 1-year period, *Atmos. Environ.*, *37*(4), 499–510, doi:10.1016/S1352-2310(02)00918-4.

Zhang, Q., et al. (2009), Asian emissions in 2006 for the NASA INTEX-B mission, *Atmos. Chem. Phys.*, *9*(14), 5131–5153, doi:10.5194/acp-9-5131-2009.

Zhi, G. R., Y. J. Chen, Y. L. Feng, S. C. Xiong, J. Li, G. Zhang, G. Y. Sheng, and J. Fu (2008), Emission characteristics of carbonaceous particles from various residential coal-stoves in China, *Environ. Sci. Technol.*, *42*(9), 3310–3315, doi:10.1021/es702247q.

Zhou, X. H., J. Cao, T. Wang, W. S. Wu, and W. X. Wang (2009), Measurement of black carbon aerosols near two Chinese megacities and the

implications for improving emission inventories, *Atmos. Environ.*, *43*(25), 3918–3924, doi:10.1016/j.atmosenv.2009.04.062.

J. Hao and Y. Wang, Ministry of Education Key Laboratory for Earth System Modeling, Center for Earth System Science, Institute for Global Change Studies, Tsinghua University, Weiqing Building, Rm. 602, Beijing 100084, China. (yxw@tsinghua.edu.cn)

M. Kajino, Meteorological Research Institute, 1-1 Nagamine, Tsukuba, Ibaraki 305-0052, Japan.

Y. Kondo, Department of Earth and Planetary Science, Graduate School of Science, University of Tokyo, Hongo 7-3-1, Bunkyo-ku, Tokyo, Tokyo 113-0033, Japan.

J. W. Munger, Department of Earth and Planetary Sciences, Harvard University, 20 Oxford St., Cambridge, MA 02138, USA.

X. Wang, School of Environment, Tsinghua University, Beijing 100084, China.